18 September 1998

ELSEVIER

Chemical Physics Letters 294 (1998) 339–344

CHEMICAL PHYSICS LETTERS

Kinetic study of gas-phase $Y(a\,^2D_{3/2})$ and $La(a\,^2D_{3/2})$ with O_2, N_2O, CO_2 and NO

Mark L. Campbell *

Chemistry Department, United States Naval Academy, Annapolis, MD 21402 USA

Received 3 June 1998; in final form 13 July 1998

Abstract

The second-order rate constants of gas-phase $Y(a\,^2D_{3/2})$ and $La(a\,^2D_{3/2})$ with O_2, N_2O, CO_2 and NO as a function of temperature are reported. In all cases, the reactions are relatively fast. For $Y(a\,^2D_{3/2})$, the bimolecular rate constants (in $cm^3\ s^{-1}$) are described in Arrhenius form by $k(O_2) = (2.2 \pm 0.1) \times 10^{-10} \exp(-3.5 \pm 0.6\ \text{kJ mol}^{-1}/RT)$, $k(N_2O) = (1.9 \pm 0.2) \times 10^{-10} \exp(-4.0 \pm 0.8\ \text{kJ mol}^{-1}/RT)$, $k(CO_2) = (1.0 \pm 0.1) \times 10^{-10} \exp(-2.3 \pm 0.6\ \text{kJ mol}^{-1}/RT)$, where the uncertainties are $\pm 2\sigma$. The rate constants for Y reacting with NO are temperature insensitive with a value of 1.0×10^{-10} $cm^3\ s^{-1}$. For $La(a\,^2D_{3/2})$, the bimolecular rate constants for all the reactants are near the gas-kinetic collision rate.

1. Introduction

The kinetics of gas-phase reactions involving transition metal (TM) atoms and oxygen-containing oxidants has recently received considerable attention [1]. TM chemistry is an intriguing field of study due to the high multiplicities of the atomic ground states and the large number of low-lying metastable states.

In this Letter we report a gas-phase kinetic study of the ground $a\,^2D_{3/2}$ states of yttrium and lanthanum with O_2, N_2O, CO_2 and NO. Parson and co-workers [2–5] have studied the Group-3 metals reacting with O_2, NO, SO_2 and ROH in crossed-beam experiments and observed the chemiluminescence of the metal oxide product. Bimolecular abstraction was established as the reaction mechanism, although absolute rate constants for these processes were not reported. In addition, LIF detection of the TM oxide product established that the Group-3 metals even abstract oxygen from aldehydes, ketones and carboxylic acids [6]. Gole and co-workers [7–9] observed YO and LaO chemiluminscence in beam-gas studies involving gas-phase yttrium and lanthanum oxidation in the presence of O_2, NO_2, N_2O and O_3. Again, bimolecular abstraction processes were indicated. The only previous rate constant measurements involving either yttrium or lanthanum in the gas phase under multiple collision conditions reported on the reactions of yttrium with small hydrocarbons [10,11]. We are unaware of any rate constant measurements involving these metals in the gas phase with oxygen-containing oxidants. This study continues our efforts to further understand the dynamics of gas-phase transition metal reactions. Although primarily phenomenological, the increase in the data base of these reactions should yield greater insight

* E-mail: campbell@brass.nadn.navy.mil

0009-2614/98/$ - see front matter
PII: S0009-2614(98)00905-1

into the important factors affecting transition metal chemistry. We hope these new kinetic results will inspire further theoretical work in an effort to gain a better understanding of these reactions.

2. Experimental

Pseudo-first-order kinetic experiments ([TM] ≪ [oxidant]) were carried out in an apparatus with slowly flowing gas using a laser photolysis/laser-induced fluorescence (LIF) technique. The experimental apparatus and technique have been described in detail elsewhere [12]. Briefly, the reaction chamber is a stainless-steel reducing 4-way cross with attached side arms and a sapphire window for optical viewing. The reaction chamber is enclosed within a convection oven (Blue M, model 206F, $T_{max} = 623$ K) for temperature dependence experiments.

Yttrium and lanthanum atoms were produced by the 248 nm photodissociation of yttrium(III) hexafluoroacetylacetonate [$Y(hfa)_3$] and tris(6,6,7,7,8,8,8-heptafluoro-2,2-dimethyl-3,5-octanedionate) lanthanum(III) [$La(FOD)_3$], respectively, using the focused output of an excimer laser (Lambda Physics Lextra 200). The photolysis laser output was focused using a lens ($f = 564$ mm) positioned approximately one focal length from the detection zone. Yttrium atoms were detected via LIF using an excimer-pumped dye laser (Lambda Physics Lextra 50/ScanMate 2E) tuned to the $y\,^2D_{5/2}{}^\circ \leftarrow a\,^2D_{3/2}$ transition at 403.983 nm and the fluorescence at 412.831 nm was isolated with an interference filter [13]. Some experiments utilized the $y\,^2F_{5/2}{}^\circ \leftarrow a\,^2D_{3/2}$ transition at 407.738 nm [13]. Experimental results were found to be independent of the optical transition employed. Lanthanum atoms were detected utilizing the $y\,^2D_{5/2}{}^\circ \leftarrow a\,^2D_{3/2}$ transition at 515.869 nm and the fluorescence at 545.515 nm was isolated with an interference filter [13]. The fluorescence was detected at 90° to the counterpropagated laser beams with a three-lens telescope imaged through an iris. A photomultiplier tube (Hamamatsu R375) was used in collecting the LIF which was subsequently sent to a gated boxcar sampling module (Stanford Research Systems SR250), and the digitized output was stored and analyzed by a computer.

Because of the low vapor pressure of the two precursors at room temperature, the precursors required heating to get enough molecules into the gas phase. Thus, the lowest temperature at which kinetic experiments could be performed corresponded to 348 K for yttrium and 373 K for lanthanum. Below these temperatures the LIF signal was too weak to measure reliable values of the rate constant.

The heated transition metal precursor was entrained in a flow of nitrogen buffer gas. The precursor carrier gas, buffer gas and reactant gases flowed through calibrated mass flow meters and flow controllers prior to admission to the reaction chamber. Each sidearm window was purged with a slow flow of nitrogen buffer gas to prevent deposition of the transition metal and other photoproducts. Pressures were measured with MKS Baratron manometers, and chamber temperatures were measured with a thermocouple. The delay time between the photolysis pulse and the dye-laser pulse was varied by a digital delay generator (Stanford Research Systems DG535) controlled by a computer. The trigger source for these experiments was scattered pump laser light incident upon a fast photodiode. LIF decay traces consisted of 200 points, each point averaged for 4 laser shots.

The following reagents were used as received: $Y(hfa)_3$ (Strem, 99.9%), $La(FOD)_3$ (Strem, 99%), O_2 (MG Industries, 99.8%), N_2O (MG Industries, electronic grade, 99.999%), CO_2 (MG Industries, anaerobic grade, 99.9%), NO (MG Industries, 99.0%) and N_2 (Potomac Airgas, 99.998%).

3. Data analysis and results

The decay rates of the $a\,^2D_{3/2}$ states of yttrium and lanthanum as a function of reactant pressure were investigated at various temperatures and total pressures. The loss of ground state atoms is described by the first-order decay constant, k_1:

$$k_1 = 1/\tau = k_o + k_2[\text{oxid}], \qquad (1)$$

where τ is the first-order time constant for the removal of the transition metal under the given experimental conditions, k_o $(= 1/\tau_o)$ is the loss term due to diffusion out of the detection zone and reaction with the precursor and precursor fragments, and k_2 is the second-order rate constant. Typical decay profiles are shown in Fig. 1. A time constant,

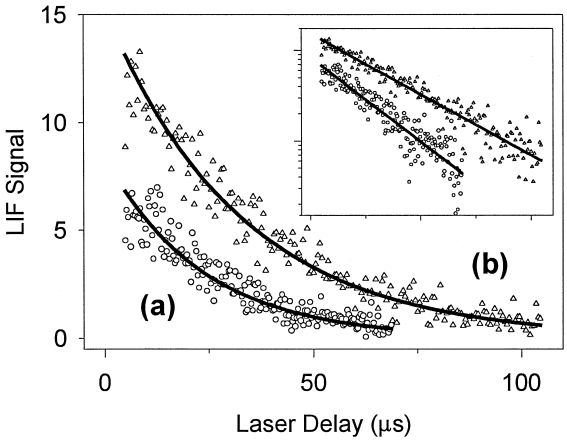

Fig. 1. Typical $Y(a^2D_{3/2})$ and $La(a^2D_{3/2})$ decay curves in the presence of O_2 at 498 K, $P_{total} = 5.0$ Torr: (a) La, $P(O_2) = 117$ mTorr, $\tau = 23.3$ μs; and (b) Y, $P(O_2) = 124$ mTorr, $\tau = 32.4$ μs. The solid lines through the data are exponential fits. The inset is a ln plot of the data.

τ, for each decay profile was determined using a linear least-squares procedure. The second-order rate constant is determined from a plot of $1/\tau$ vs. reactant number density. Typical plots for obtaining second-order rate constants are presented in Fig. 2; the slope yields the observed rate constant. The relative uncertainty (i.e., the reproducibility) of the second-order rate constants is estimated at $\pm 20\%$ based on repeated measurements of rate constants under identical temperature and total pressure conditions. The absolute uncertainties are estimated to be $\pm 30\%$ and

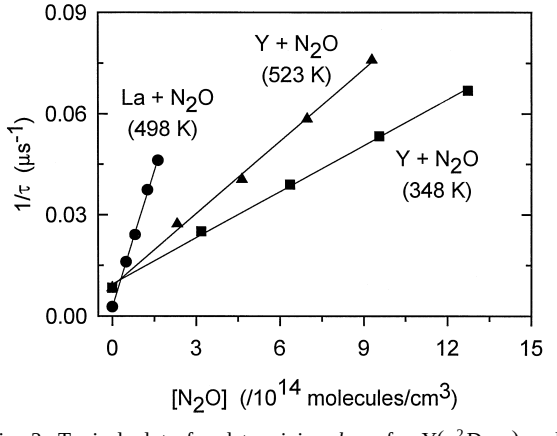

Fig. 2. Typical plots for determining k_{2nd} for $Y(a^2D_{3/2})$ and $La(a^2D_{3/2})$. The solid line for each set of data is a linear regression fit from which k_{2nd} is obtained.

are based on the sum of the statistical scatter in the data, uncertainty in the flowmeter and flow controller readings (5%) and the total pressure reading (1%), and uncertainties due to incomplete gas mixing and incomplete relaxation of excited states produced in the photolysis event.

3.1. Reactions of $Y(a^2D_{3/2})$

Second-order rate constants for the $a^2D_{3/2}$ state reacting with O_2, N_2O, CO_2 and NO at a total pressure of 5 Torr from 373 to 548 K are listed in Table 1. Rate constants could not be measured above 548 K due to thermal decomposition of the precursor. The rate constants at 373 K for these reactions were also measured at a total pressure of 20 Torr and are independent of total pressure within experimental uncertainty.

The rate constants (in $cm^3\ s^{-1}$) are described in Arrhenius form by:

$$k(O_2) = (2.2 \pm 0.1) \times 10^{-10} \times \exp(-3.5 \pm 0.6\ \text{kJ mol}^{-1}/RT), \quad (2)$$

$$k(N_2O) = (1.9 \pm 0.2) \times 10^{-10} \times \exp(-4.0 \pm 0.8\ \text{kJ mol}^{-1}/RT), \quad (3)$$

$$k(CO_2) = (1.0 \pm 0.1) \times 10^{-10} \times \exp(-2.3 \pm 0.6\ \text{kJ mol}^{-1}/RT), \quad (4)$$

where the uncertainties are $\pm 2\sigma$. The reaction with NO is temperature independent within experimental error.

Table 1
Second-order rate constants[a] ($/10^{-10}$ $cm^3\ s^{-1}$) for the $a^2D_{3/2}$ state of yttrium with O_2, N_2O, CO_2 and NO at a total pressure of 5 Torr

T (K)	O_2	N_2O	CO_2	NO
348	0.61	0.45	0.43	1.0
373	0.73	0.54	0.49	1.1
398	0.75	0.55	0.49	1.0
423	0.78	0.60	0.52	1.0
448	0.88	0.70	0.56	0.92
473	0.88	0.69	0.53	1.0
498	0.92	0.72	0.58	1.0
523	0.95	0.73	0.58	1.0
548	0.99	0.76	0.59	1.0

[a] Uncertainties are $\pm 30\%$.

Table 2
Second-order rate constants[a] ($/10^{-10}$ cm^3 s^{-1}) for the $a^2D_{3/2}$ state of lanthanum with O_2, N_2O, CO_2 and NO at a total pressure of 5 Torr

T (K)	O_2	N_2O	CO_2	NO
373	1.5	2.3	1.9	1.9
398	1.5	2.1	1.8	1.8
423	1.7	2.2	1.9	1.9
448	1.7	2.3	2.1	1.9
473	1.6	2.1	1.9	1.7
498	2.0	2.6	2.2	2.1
523	2.0	2.8	2.4	2.3

[a]Uncertainties are $\pm 30\%$.

3.2. Reactions of La($a^2D_{3/2}$)

Second-order rate constants for the $a^2D_{3/2}$ state reacting with O_2, N_2O, CO_2 and NO at a total pressure of 5 Torr from 373 to 523 K are listed in Table 2. The rate constants at 373 K for these reactions were also measured at a total pressure of 20 Torr and are independent of total pressure within experimental uncertainty.

The rate constants for lanthanum with all the reactants are near the gas-kinetic collision rate, indicating barriers to reaction are negligible. The slight increase in the rate constants for all the reactions can be accounted for as arising from the increased collision frequency of the reactants at higher temperatures.

4. Discussion

Unfortunately, little is known about the potential energy surfaces for the interaction of transition metal atoms with even the simplest of molecules. A complete understanding of these reactions awaits advances in theoretical dynamics calculations for these systems. Nevertheless, it is still useful to assess the experimental data reported thus far to look for general trends and correlations between the reaction rates and the physical properties of the transition metal.

4.1. Y + OX

The pressure independence observed for these reactions indicates termolecular processes are unimportant. We did not attempt to directly observe the YO product molecule; however, YO has been observed previously for these reactions by other groups [2,3,5,7,9]. Thus, bimolecular abstraction of an oxygen atom to produce YO is the indicated reaction mechanism. The exothermicities for production of YO on the ground state surface for the reactions of yttrium with O_2, N_2O, CO_2 and NO are 211, 542, 177, and 78 kJ mol^{-1}, respectively [14]; thus, no thermodynamic barriers exist for these reactions. The experimentally measured kinetic barriers for all these reactants are small (< 5 kJ mol^{-1}), and in every case reaction occurs on average in fewer than 10 hard-sphere collisions. The 4d series appears to be the most reactive of the transition metal series. This reactivity has been ascribed to the similar size and relative energies of the 5s and 4d subshells. These similarities allow the d orbitals to be more involved in the bonding yielding a more attractive potential in the entrance channel [10,15].

4.2. La + OX

As with the yttrium reactions, bimolecular abstraction of an oxygen atom to produce LaO is indicated for these oxidants based on the pressure independence of the rate constants and the detection of the LaO product by other groups [2,5,8]. The production of LaO is exothermic for all the oxygen-containing oxidants reported here. The exothermicities for the reactions of ground state lanthanum with O_2, N_2O, CO_2 and NO are 303, 634, 269 and 170 kJ mol^{-1}, respectively [14]; thus, no thermodynamic barriers exist for these reactions. The reactions of lanthanum with all the reactants studied here are near the gas-kinetic collision rate. Thus, lanthanum is one of the most reactive of the TMs in reactions with oxygen-containing molecules, and its reactions with oxygen-containing oxidants are considerably faster than the reactions of the other TMs in the 5d series [1].

The only TM more reactive with these oxidants than lanthanum is niobium [16]. Niobium's reactivity has been attributed to its lone valence s electron in the 5s subshell. Lanthanum is the most reactive of all the TMs with $s^2 d^{n-2}$ configurations.

The reactivity of lanthanum might be due to its small ionization energy, i.e., lanthanum has the low-

est ionization energy of all the TMs [17]. An electron transfer model has been proposed to explain rate constants of TMs in O-atom abstraction reactions [18]. The small ionization energy of lanthanum might facilitate electron transfer from the metal atom to the oxidant which consequently results in fast reactions.

Lanthanum is unique among the 5d series TM atoms because of its lack of a filled 4f subshell. Lanthanum is not affected by the lanthanide contraction so its size is considerably larger and its ionization energy smaller than the other 5d TM atoms. Thus, it is not surprising that the unique nature of the electronic structure of lanthanum relative to the other 5d TM metals results in its anomalous reactivity.

With the completion of these kinetic measurements for yttrium and lanthanum, all the exothermic abstraction reactions involving TMs with O_2 have now been reported. Table 3 tabulates the room-temperature rate constants for these reactions along with the ionization energy and reaction enthalpies. There appears to be no relation to the kinetics of these processes and the enthalpy of reaction. However, within a TM series there appears to be a modest correlation between the ionization energy and the rate constant. The three atoms of the 3d series show an inverse relationship between ionization energy and the rate constant. The deviations from this trend in the 4d series are complicated by the electronic configurations of niobium and molybdenum. Both atoms have $s^1\,d^{n-1}$ configurations which make these atoms exceptionally reactive. The only exception to this trend in the 5d series is rhenium, the least reactive of all the TMs which involve exothermic abstraction processes. Hopefully, advances will be made in dynamics calculations so that the variations in the rate constants for these reactions can be better understood.

Fontijn and co-workers have advanced a resonance interaction model [29] to predict barriers to reaction and rate constants for metal atoms reacting with N_2O. In this model, the activation barriers are calculated by taking into account the ionization energy and sp promotion energy of the metal, the electron affinity of N_2O, and the bond energy of the metal oxide product. The resonance interaction model predicts the energy barriers for the reactions of yttrium and lanthanum with N_2O to be 2.2 and 0.0 kJ mol^{-1} [29], respectively. These values are very close to the measured values, although the predictive ability of this model has not been as accurate for other transition metals [1].

5. Summary

We have measured bimolecular reaction rate constants and Arrhenius parameters for the reactions of

Table 3
Ionization energies, enthalpies of reaction and room-temperature rate constants for the reaction: $TM(g) + O_2(g) \rightarrow TMO(g) + O(g)$

Metal	IE[a] (eV)	ΔH^{o} [b] (kJ mol^{-1})	k_{2nd} ($/10^{-11}$ cm^3 s^{-1})	Ref.
$Sc(s^2\,d^1\,^2D_{3/2})$	6.561	−183	0.61	[18,19]
$Ti(s^2\,d^2\,^3F_2)$	6.828	−170	0.16	[20–22]
$V(s^2\,d^3\,^4F_{3/2})$	6.746	−139	0.31	[18,23]
$Y(s^2\,d^1\,^2D_{3/2})$	6.217	−211	5.4[c]	this work
$Zr(s^2\,d^2\,^3F_2)$	6.634	−297	2.0	[1]
$Nb(s^1\,d^4\,^6D_{1/2})$	6.759	−285	25	[16]
$Mo(s^1\,d^5\,^7S_3)$	7.092	−99	11	[24,25]
$La(s^2\,d^1\,^2D_{3/2})$	5.577	−303	13.[c]	this work
$Hf(s^2\,d^2\,^3F_2)$	6.825	−320	3.7	[1]
$Ta(s^2\,d^3\,^4F_{3/2})$	7.89	−340	0.73	[26]
$W(s^2\,d^4\,^5D_0)$	7.98	−177	0.16	[12]
$Re(s^2\,d^5\,^6S_{5/2})$	7.88	−125	0.018	[27]
$Os(s^2\,d^6\,^5D_4)$	8.7	−34	0.071[c]	[28]

[a] Ref. [17].
[b] Ref. [14].
[c] Value obtained by extrapolation to 298 K.

the $a\,^2D_{3/2}$ state of yttrium and lanthanum with O_2, N_2O, CO_2 and NO. In each case, abstraction of an oxygen atom to produce the transition metal oxide is the reaction channel. The activation barriers for all these reactions are small ($E_a < 5$ kJ mol^{-1}).

Acknowledgements

This research was supported by a Cottrell College Science Award of Research. Acknowledgment is made to the Donors of the Petroleum Research Fund, administered by the American Chemical Society, for partial support of this research. The author is a Henry Dreyfus Teacher–Scholar.

References

[1] M.L. Campbell, J. Chem. Soc., Faraday Trans. 94 (1998) 1687, and references cited therein.
[2] D.M. Manos, J.M. Parson, J. Chem. Phys. 63 (1975) 3575.
[3] K. Liu, J.M. Parson, J. Chem. Phys. 67 (1977) 1814.
[4] K. Liu, J.M. Parson, J. Chem. Phys. 68 (1978) 1794.
[5] D.M. Manos, J.M. Parson, J. Chem. Phys. 69 (1978) 231.
[6] K. Liu, J.M. Parson, J. Phys. Chem. 83 (1979) 970.
[7] C.L. Chalek, J.L. Gole, J. Chem. Phys. 65 (1976) 2845.
[8] J.L. Gole, C.L. Chalek, J. Chem. Phys. 65 (1976) 4384.
[9] C.L. Chalek, J.L. Gole, Chem. Phys. 19 (1977) 59.
[10] J.J. Carroll, K.L. Haug, J.C. Weisshaar, J. Am. Chem. Soc. 115 (1993) 6962.
[11] J.J. Carroll, K.L. Haug, J.C. Weisshaar, M.R.A. Blomberg, P.E.M. Siegbahn, M. Svensson, J. Phys. Chem. 99 (1995) 13955.
[12] M.L. Campbell, R.E. McClean, J. Chem. Soc., Faraday Trans. 91 (1995) 3787.
[13] W.F. Meggers, C.H. Corliss, B.F. Scribner, Tables of Spectral-Line Intensities, Part 1 Arranged by Elements, Natl. Bur. Stand. Monogr. 145, U.S. Gov. Print. Off., Washington, DC, 1975.
[14] D.D. Wagman, W.H. Evans, V.B. Parker, R.H. Schumm, I. Halow, S.M. Bailey, K.L. Churney, R.L. Nuttall, The NBS tables of chemical thermodynamic properties, J. Phys. Chem. Ref. Data 11 (1982) Suppl. 2.
[15] J.J. Carroll, J.C. Weisshaar, J. Phys. Chem. 100 (1996) 12355.
[16] R.E. McClean, M.L. Campbell, E.J. Kölsch, J. Phys. Chem. A 101 (1997) 3348.
[17] D.R. Lide (Ed.), CRC Handbook of Chemistry and Physics, 75th ed., CRC Press, Boca Raton, FL, 1995.
[18] D. Ritter, J.C. Weisshaar, J. Phys. Chem. 94 (1990) 4907.
[19] M.L. Campbell, K.L. Hooper, E.J. Kölsch, Chem. Phys. Lett. 274 (1997) 7.
[20] D. Ritter, J.C. Weisshaar, J. Phys. Chem. 93 (1989) 1576.
[21] M.L. Campbell, R.E. McClean, J. Phys. Chem. 97 (1993) 7942.
[22] D.E. Clemmer, K. Honma, I. Koyano, J. Phys. Chem. 97 (1993) 11480.
[23] R.E. McClean, L. Pasternack, J. Phys. Chem. 96 (1992) 9828.
[24] L. Lian, S.A. Mitchell, D.M. Rayner, J. Phys. Chem. 98 (1994) 11637.
[25] M.L. Campbell, R.E. McClean, J.S.S. Harter, Chem. Phys. Lett. 235 (1995) 497.
[26] M.L. Campbell, K.L. Hooper, J. Chem. Soc., Faraday Trans. 93 (1997) 2139.
[27] M.L. Campbell, J. Phys. Chem. A 102 (1998) 892.
[28] M.L. Campbell, J. Phys. Chem. 100 (1996) 19430.
[29] P.M. Futerko, A. Fontijn, J. Chem. Phys. 95 (1991) 8065.